Late Quaternary insolation forcing on total organic carbon and C37 alkenone variations in the Arabian Sea

Dörte Budziak, Ralph R. Schneider, Frauke Rostek, Peter J. Müller, Edouard Bard, Gerold Wefer

PALEOCEANOGRAPHY, VOL. 15, NO. 3, PAGES 307-321, JUNE 2000

Late Quaternary insolation forcing on total organic carbon and C_{37} alkenone variations in the Arabian Sea

Dörte Budziak,[1] Ralph R. Schneider,[1] Frauke Rostek,[2] Peter J. Müller,[1]
Edouard Bard,[2] and Gerold Wefer[1]

Abstract. We here present records of total organic carbon (TOC) and C_{37} alkenones, used as indicators for past primary productivity, from the western (WAS) and eastern Arabian Sea (EAS). New data from an open ocean site of the WAS upwelling area are compared with similar records from Ocean Drilling Program (ODP) Site 723 from the continental margin off Oman and MD 900963 from the EAS. These records together with other proxies used to reconstruct upwelling intensity, indicate periods of high productivity in tune with precessional forcing. On the basis of their phase relationship to boreal summer insolation they can be divided into three groups: in the WAS differences between monsoonal proxies (1) and productivity (2) document a combined signal of moderate SW monsoon winds and of strengthened and prolonged NE monsoon winds, whereas in the EAS phasing indicates maximum productivity (3) at times of stronger NE monsoon winds associated with precession-related maxima in ice volume.

1. Introduction

Deep-sea sediment records from the Arabian Sea document the history of the monsoonal circulation in the Indian Ocean. Various studies on wind-transported material such as land-derived pollen spectra [*Van Campo et al.,* 1982] and dust input [*Clemens and Prell,* 1990, 1991; *Sirocko et al.,* 1993] from adjacent landmasses, as well as proxy records of surface water productivity [e.g., *Prell and Kutzbach,* 1987; *Naidu and Malmgren,* 1996; *Reichart et al.,* 1998] revealed a strong link between precessionally driven insolation changes and monsoon intensity. This is in agreement with results from general circulation models (GCM) [e.g., *Prell and Kutzbach,* 1987, 1992; *DeMenocal and Rind,* 1993] pointing to an intensification of SW monsoon winds and enhanced upwelling with increased boreal summer insolation. Additionally, in the precessional frequency band, *Clemens et al.* [1991] documented a time lag of ~ 8 kyr (about -120° on average) between maximum boreal summer insolation (referenced to June 21) and various indicators of SW monsoon winds and related upwelling intensity. Thus radiative forcing alone cannot account for the timing of strong monsoons. *Clemens et al.* [1991] concluded that this time lag is phase-locked to the cross-equatorial transport and release of latent heat over the Tibetan Plateau resulting in intensified summer monsoon winds.

In the northern Arabian Sea, *Reichart et al.* [1998] used a variety of productivity proxies, e.g., variations of total organic carbon (TOC), to examine variations in the Indian monsoon system, applying an age model independent of the Spectral Mapping Project (SPECMAP) reference stack [*Imbrie et al.,* 1984]. Their results indicate that precession-related productivity maxima lag boreal summer insolation maxima by ~ 6 kyr (about -94°) on average. This lag is attributed to a prolonged summer monsoon season linked to late instead of early summer insolation [*Reichart et al.,* 1998].

In contrast, sediments from shallower sites at the continental slope off Oman seem to be more influenced by changes in climatic boundary conditions associated with glacial-interglacial cycles due to sea level changes and resulting sea-landward shifts of the coastal upwelling cells [*Emeis,* 1993]. Accordingly, data from Ocean Drilling Program (ODP) Site 723 suggested that the SW monsoon was weakened during glacial times as compared to the interglacials [*Niitsuma et al.,* 1991; *Anderson and Prell,* 1993]. This was interpreted to result from a glacial reduction of the pressure gradient between the ice-covered Tibetan Plateau and the Indian Ocean [*Prell,* 1984]. Consequently, the authors concluded that upwelling and the resulting primary production were reduced during cold climate periods.

In addition, paleoproductivity records revealed a different phasing with respect to boreal summer insolation between the western (WAS) and eastern Arabian Sea (EAS). *Emeis* [1993] used TOC accumulation rates to reconstruct paleoproductivity at ODP Site 723. The precessional component in this record, though of minor importance at this site, indicates a rather opposite phasing +10.7 kyr (+167°) [*Emeis,* 1993], while in the EAS a paleoproductivity reconstruction based on the coccolithophorid *Florisphaera profunda* showed a lead of +7.7 kyr (+120°) with respect to maximum summer insolation [*Beaufort et al.,* 1997]. Therefore these former studies raise two questions: (1) How important is the 100 kyr cycle, and (2) what is the reason for the difference in the phasing of primary productivity records relative to precession and insolation changes?

In order to reassess the different phasing of TOC variations and related paleoproductivity in the Arabian Sea, we here

[1]Fachbereich Geowissenschaften, Universität Bremen, Bremen, Germany.
[2]Centre Européen de Reserche et d'Enseignement en Géosciences de l'Environment (CEREGE), Université d'Aix-Marseille III et CNRS-UMR 6635, Europôle de l'Arbois, Aix-en-Provence, France.

Paper number 1999PA000433.
0883-8305/00/1999PA000433$12.00

present new data of TOC and C_{37} alkenone (C_{37}) variations of core GeoB 3005, an open ocean site from within the upwelling area of the WAS (14°58.3'N, 54°22.2'E; 2310 m), in combination with ODP Site 723 (18°03.079'N, 57°36.561'E; 816 m) [*Emeis,* 1993; *Emeis et al.,* 1995] and MD 900963 from the EAS (05°04'N, 73°53'E; 2450 m) [*Rostek et al,* 1994, 1997].

2. Monsoon Meteorology and Hydrographic Setting

The dominant component of tropical climate variability in the Arabian Sea is the seasonal reversal of atmospheric circulation and precipitation associated with the Asian monsoon system. The distribution of a continental landmass in the north and a large ocean in the south leads to this reversal of air flow [*Cadet,* 1979]. During the Northern Hemisphere's Summer the southern Asian continent heats up more than the Indian Ocean. This extra heating causes a low-pressure cell over the Tibetan Plateau and a pressure high above the Indian Ocean. The formation of a strong, low-level jet stream known as the Findlater Jet [*Findlater,* 1969] is the result. Latent heat, absorbed over the southern subtropical ocean, transported northward across the equator, and released by precipitation over the Indian continent, controls the intensity of this jet [e.g., *Webster,* 1987].

The strong coupling between atmosphere and ocean and the seasonal changes in wind direction as well as wind intensities cause a complete semiannual reversal of surface currents in the Arabian Sea basin affecting primary productivity. *Haake et al.* [1993] described enhanced fluxes during both the SW and NE monsoon seasons. Lower fluxes were observed during the intermonsoon seasons in the WAS and central Arabian Sea (CAS), whereas peak fluxes in the EAS do not start until the late SW monsoon period, which lasts until the end of October [*Haake et al.,* 1993]. Here particle fluxes are more variable during the rest of the year. On average, highest biogenic flux rates occur in the WAS, and lower fluxes occur in the CAS and EAS. *Rixen et al.* [1996] observed that at least in the WAS, particle fluxes are controlled not only by the intensity of the upwelling systems but additionally by the amount of cold, nutrient-poor water masses which are transported from south of the equator into the upwelling region off Oman, where highest fluxes occur during SW monsoons with moderate wind speeds.

During the summer season, coastal upwelling develops off the Somali and Oman coasts [*Wyrtki,* 1973] because of Ekman transport. As the SW monsoon winds, blowing parallel to the coast with the coast on its left (Figure 1), drive the ocean circulation, surface water is transported offshore and replaced by colder, nutrient-rich subsurface water masses within a narrow band (100 km) along the coast. Farther offshore, an open ocean-type upwelling develops in a broad region (400 km) because of the positive curl in the wind stress [*Swallow,* 1984; *Luther et al.,* 1990; *Brock and McClain,* 1992]. Along the west coast of India, weak upwelling may occur under favorable conditions [*Wyrtki,* 1973]. Long-time sediment trap studies report an increase in biogenic and lithogenic particle fluxes with the onset of the summer monsoon in correlation with higher wind speeds and decreasing sea surface temperatures in the WAS and EAS [*Nair et al.,* 1989; *Ittekkot et al.,* 1992; *Haake et al.,* 1993].

With the cooling of the Tibetan Plateau the atmospheric pressure gradient reverses and initiates the winter monsoon. A moderate, cool NE monsoon wind (Figure 1) compensates the pressure gradient between a now persisting high-pressure cell above the snow-covered Tibetan Plateau and a pressure low over the Indian Ocean [e.g., *Hastenrath and Lamb,* 1979]. During the 1995 U.S. Joint Global Ocean Flux Study (JGOFS) Arabian Sea Process Study, *Hansell and Peltzer* [1998] examined TOC concentrations in the upper ocean. They described highest TOC concentrations in the mixed layer during the NE monsoon period remaining through to mid summer, while lowest TOC concentrations in the mixed layer occurred in late summer.

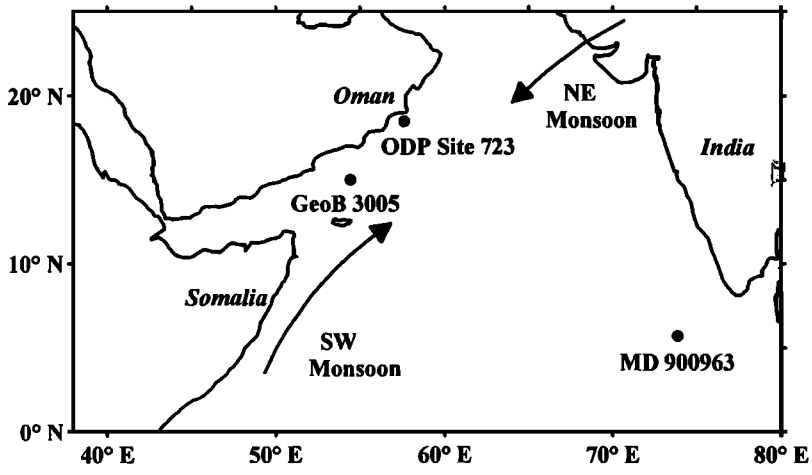

Figure 1. Map of the Indian Ocean north of the equator. Indicated are the locations of cores GeoB 3005, Ocean Drilling Program (ODP) Site 723, and MD 900963. Arrows show major wind directions of the Indian Monsoon system during summer (SW monsoon) and winter seasons (NE monsoon)

3. Material and Methods

3.1. Material

During *R/V Meteor* cruise M31/3 a gravity core (GeoB 3005-1, water depth 2316 m), a piston core (GeoB 3005-2, water depth 2309 m), and a multicorer core (GeoB 3005-3, water depth 2316 m) were recovered from a station within the upwelling area in the WAS (14°58.3'N, 54°22.2'E, site 108 in the work of *Hemleben et al.* [1996]). To minimize possible effects caused by lateral sediment transport from the continental margin, the site was positioned on a submarine plateau. GeoB 3005-1 was sampled over its entire length (1098 cm) at 5 cm intervals with 10 mL syringes and GeoB 3005-2 only between 748 and 1948 cm. These samples were stored at 4°C. GeoB 3005-3 was sampled in 1 cm slices on board, and the samples were stored frozen.

3.2. Methods

One sample series of the cores from station GeoB 3005 was wet sieved to obtain the coarse fraction (> 63 μm) which was used to pick the planktonic foraminiferal species *Neogloboquadrina dutertrei* (d'Orbigny) for stable oxygen isotope ($\delta^{18}O$) measurements. The samples were analyzed using a Finnigan MAT 251 micromass spectrometer coupled with a Finnigan automated carbonate device. The carbonate was reacted with 100% orthophosphoric acid at 75°C. The reproducibility (1 σ) based on replicate measurements of a laboratory internal carbonate standard (Solnhofen limestone) is +/- 0.07 ‰

A second sample series was freeze-dried, ground in an agate mortar, and used for carbon and alkenone analyses. Organic carbon was determined on decalcified samples by combustion at 1050°C using a Heraeus CHN-O-Rapid elemental analyzer [*Müller et al.*, 1994]. The precision of the measurements was better than 3% on the basis of duplicates and a laboratory internal reference sediment (WS2).

The concentrations of C_{37} alkenones (long-chain unsaturated ketones, which are biosynthesized by coccolithophorids of the class *Haptophytes* [*Volkman et al.*, 1995]) were determined in 2 g aliquots of freeze-dried sediment samples. The samples were extracted with a UP200H ultrasonication disruptor probe (S3 micropoint, amplitude 0.5, and pulse 0.5) and successively less polar solvent mixtures (MeOH, MeOH/CH_2Cl_2 (1:1), and CH_2Cl_2), each for 3 min. The extracts were combined, washed with demineralized water to remove sea salt and methanol, dried over Na_2SO_4, concentrated under N_2, and finally taken up in 25 μL of a 1:1 (volume) MeOH/CH_2Cl_2 mixture.

3 μL aliquots of the final extracts were analyzed by capillary gas chromatography using a HP 5890 Series II gas chromatograph (GC) equipped with a 50 m x 0.32 mm inner diameter (ID) HP Ultra 1 (cross-linked methyl silicone) fused silica column, a split injector (1:10), and a flame ionisation detector. Helium was used as carrier gas. The GC was programmed from 50° to 150°C at 30°C/min, 150° to 230°C at 8°C/min, and 230° to 320°C at 6°C/min, followed by an isothermal period of 45 min. Quantification of C_{37} alkenones was achieved by an internal standard method using octacosane acid methyl ester (OCSME) and the relative response factor of the C_{38} *n*-alkane as internal standards.

To avoid dilution effects caused by changes in the sedimentation rate due to varying input of terrigenous detritus and other major biogenic components (e.g., carbonate when considering the TOC and alkenone fluctuations), mass accumulation rates of TOC (TOC MAR) and C_{37} (C_{37} MAR) were calculated for all cores: The concentrations of TOC and C_{37} were multiplied with the dry bulk density of the sediments and the linear sedimentation rates between stratigraphic tie-points.

To correlate the last 300 kyr with a record from the EAS, core sampling of MD 900963 was extended to a depth of 1720 cm. For the extended part of MD 900963, TOC was determined using a NA 1500 (FISONS) elemental analyzer. Samples were treated using the method described by *Verardo et al.* [1990]. Sample preparation and technical details used at Centre Européen de Reserche et d'Enseignement en Géosciences de l'Environment (CEREGE) for extending the alkenone record of core MD 900963 are given elsewhere [*Sonzogni et al.*, 1997]. Sample treatment and determination of TOC and alkenone data of ODP Site 723, provided by K.-C. Emeis, were previously described in detail by *Emeis* [1993].

The software program SPECTRUM developed by *Schulz and Stattegger* [1997] was used to identify the dominant frequencies in the records of $\delta^{18}O$, TOC, TOC MAR, C_{37}, and C_{37} MAR and to carry out cross-spectral analyses. Because of an internal algorithm this software does not need equidistant time series. To prove the statistical significance, a Fischer/Siegel test was employed in the subroutine „Harmonic". The same parameters were used in these calculation procedures (level of significance is 0.05, Oversampling Factor (OFAC) is 4, and High Frequency Factor (HIFAC) is 1). For a more precise evaluation of temporal correspondence between boreal summer insolation and TOC time series, cross-spectral analyses were performed. This method does not only include an estimation of coherency, a linear correlation coefficient in the spectral domain, but also estimates the lead (+) or lag (-) reported as phase angles between +180° and -180°, respectively, between records sharing a similar variance at a given frequency [*Jenkins and Watts*, 1968; *Imbrie et al.*, 1989].

Three records of Northern Hemisphere summer insolation were generated for June 21 at 30°N after *Berger* [1978], with time resolutions of 2.5, 1.6, and 0.75 kyr in accordance with the mean time resolutions of the TOC records from ODP Site 723, MD 900963 and GeoB 3005, respectively. The calculation procedure of the cross-spectral analyses was also kept constant for all records (level of significance is 0.1, OFAC is 4, HIFAC is 1; window type is Welch, and 2 segments with 50% overlap; see *Schulz and Stattegger* [1997] for further details).

4. Stratigraphy

The $\delta^{18}O$ records of the planktonic foraminifera *N. dutertrei* of GeoB 3005-1 (gravity core), GeoB 3005-2 (piston core), and GeoB 3005-3 (multicorer core) were used to combine these three cores and to build a stratigraphic framework. The gravity and piston cores were brought together within an overlapping section from 938 to 1158 cm

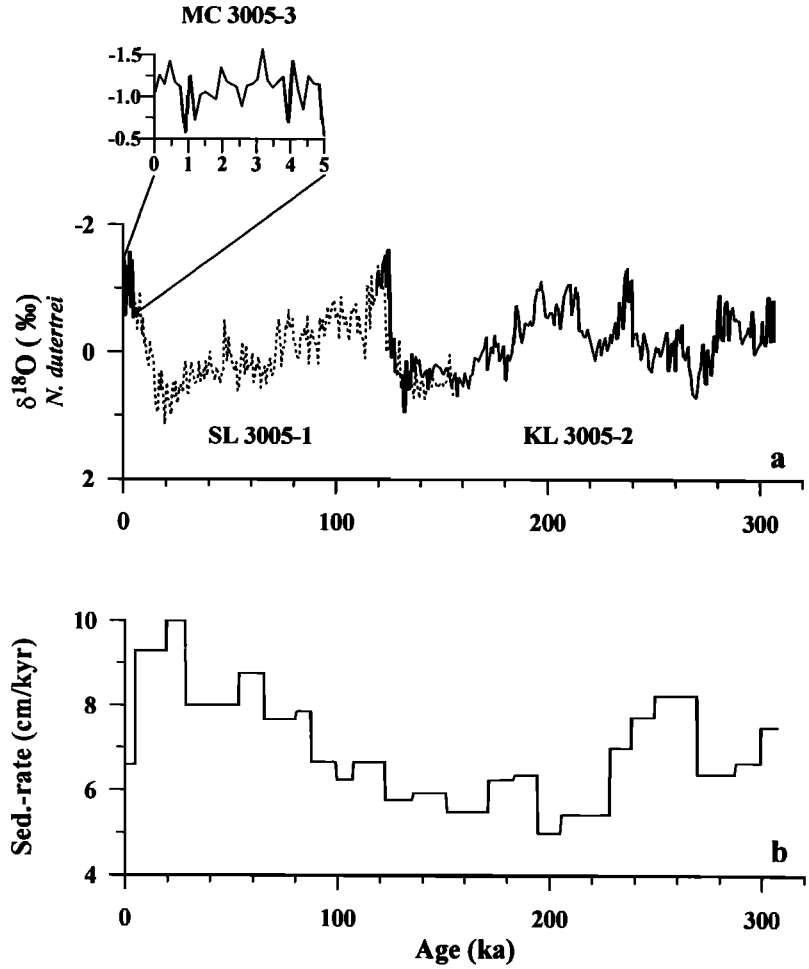

Figure 2. (a) Combination of GeoB cores 3005-1 and 3005-2 within an overlapping section (119 to 156 kyr). GeoB 3005-3 was set on top. Isotopic events (Table 1) were used as stratigraphic control points. (b) Linear sedimentation rates derived from this age model.

(original core depth) by peak to peak correlation. On the basis of both the isotopic and TOC records, GeoB 3005-3 was set on top of the stacked cores (Figure 2a). Zero age is assumed for the multicorer surface. Afterward, for the sake of homogeneity with a common timescale, the stable oxygen isotope record of *N. dutertrei* was correlated to the widely used marine oxygen isotope stages (MIS) of the SPECMAP $\delta^{18}O$ stack (Table 1) [*Imbrie et al.*, 1984] using the software program AnalySeries 1.0a7 [*Paillard et al.*, 1996].

According to our age model, the composite sediment record at site GeoB 3005 resolves the last 307 kyr, showing an average sedimentation rate of ~ 7 cm/kyr. The linear sedimentation rates were calculated between stratigraphic tie-points and range from 5 cm/kyr in MIS 7 up to 10 cm/kyr in MIS 2, as shown in Figure 2b. Thus the mean time resolution of samples taken at intervals of 5 cm lies between 500 and 1000 years.

The $\delta^{18}O$ signals of the planktonic foraminiferal species *Pulleniatina obliquiloculata* and *Globigerinoides ruber* were used to establish the stratigraphic framework of ODP Site 723 [*Niitsuma et al.*, 1991; *Emeis*, 1993; *Emeis et al.*, 1995] and of core MD 900963 [*Bassinot et al.*, 1994], respectively.

5. Results

5.1. Western Arabian Sea, Open Ocean: GeoB 3005

The $\delta^{18}O$ signal of the planktonic foraminifera *N. dutertrei* (Figure 3) reflects the typical late Quaternary pattern of global glacial to interglacial climate changes. In contrast, the records of TOC and C_{37} (Figure 3), paralleling each other, reach maximum values every 20 to 25 kyr. Except for the high values during the Holocene, probably because of lacking diagenetic equilibrium, TOC ranges between 0.4 and 2.1%. The absolute concentration of C_{37} shows pronounced variations between 400 and 6900 ng/g dry sediment. During the Holocene the alkenone content remains relatively low.

TOC MAR and C_{37} MAR of GeoB 3005 show variations between 0.2 and 1.31 g/m^2 per year, and 14 and 356 μg/m^2 per year, respectively. The pronounced periodicity with minimum and maximum values occurring during glacial as well as interglacial stages every 20 to 25 kyr are still obvious in the TOC MAR and C_{37} MAR of GeoB 3005.

In the variance power spectrum the $\delta^{18}O$ signal (Figure 4) exhibits peaks at periods (1/frequency) of 112, 40, and 23 kyr

Table 1. Isotopic Events Used as Stratigraphic Control Points From Correlation of the Timescale of the Spectral Mapping Project (SPECMAP) With GeoB 3005

Event	Time, kyr	Depth, cm
Sediment Surface	0	0.5
2	12	98
2.2	19	163
3.1	28	253
3.3	53	453
4.2	65	558
5.1	80	673
5.2	87	728
5.3	99	808
5.4	107	858
5.5	122	958
6.2	135	1033
6.4	151	1128
6.5	171	1238
6.6	183	1313
7.1	194	1383
7.2	205	1438
7.4	228	1563
7.5	238	1633
8.2	249	1718
8.4	269	1883
8.5	287	1998
8.6	299	2078
End of core	307	2138

SPECMAP is from *Imbrie et al.* [1984], and GeoB 3005 is in centimeters.

in the eccentricity, obliquity, and precessional bands, respectively, with decreasing variance toward the higher frequencies. Periodicities > 100 kyr have to be interpreted with caution because of the relative shortness of the time series of GeoB 3005, but they clearly indicate that the $\delta^{18}O$ record reflects the global changes in sea water $\delta^{18}O$ due to the buildup and retreat of continental icemasses and changes in sea surface temperatures during the last 307 kyr.

A different distribution of variance is revealed in the time series of TOC and C_{37} (Figure 4). Dominant variance is concentrated within the precession band of both records. Only TOC reveals a significant peak in the obliquity band. Variance in the low-frequency domain of eccentricity is present in C_{37} but is of only secondary importance in the TOC record. The overall dominance of the 23 kyr periodicity in the TOC and C_{37} records indicates a precessionally related forcing rather than changes in the glacial boundary conditions. The results of the spectral analyses of TOC MAR and C_{37} MAR (Figure 4) are in accordance with TOC and C_{37}, which indicates that changes in the sedimentation rate do not significantly influence these signals at this site.

5.2. Western Arabian Sea, Continental Slope off Oman: ODP Site 723

For comparison with a coastal upwelling site in the WAS we here reconsider results from ODP Site 723 [*Emeis,* 1993; *Emeis et al.,* 1995]. Variations of TOC (Figure 5) range between 0.5 and 7.5%. At ODP Site 723, TOC values are consistently higher during interglacial periods [*Emeis,* 1993; *Emeis et al.,* 1995] (Figure 5). Superimposed on these fluctuations in the low-frequency domain are variations which indicate, similar to GeoB 3005, periodic increases at time intervals of ~ 20 to 25 kyr. These are still evident within the TOC MAR (0.8 to 13 g/m^2 per year) (Figure 5), although ODP Site 723 exhibits intervals of very high TOC accumulation around 10 to 20 kyr, 60 to 80 kyr, and 130 to 150 kyr corresponding to the glacial maxima in MIS 2, 4, and 6, respectively [*Emeis et al.,* 1995]. The difference between glacial and interglacial sedimentation rates seems to be less pronounced in sediments older than MIS 6, when TOC and TOC MAR show a more parallel progress [*Emeis,* 1993; *Emeis et al.,* 1995].

At ODP Site 723 the concentrations of C_{37} (Figure 5) range between 47 and 4508 ng/g dry sediment, and thus are rather low compared to the other sites. In contrast, C_{37} MAR (Figure 5) (5 to 1158 μg/m^2 per year) is higher than in the WAS and EAS open ocean sites. Variations of C_{37} and C_{37} MAR are in good accordance with each other, while higher amounts of C_{37} are revealed in glacial stages 8 to 4, following more closely the pattern of TOC MAR.

The results of the spectral analyses of TOC (Figure 7) show the major peak in the eccentricity band and decreasing variance toward the higher frequencies, while TOC MAR is dominated by variance in the obliquity band. Although of minor importance at this site, variance in the precessional frequency band is still present. In contrast to ODP Site 723, the productivity records of GeoB 3005 have varied in tune with precessional forcing but have no clear 41 kyr cyclicity.

5.3. Eastern Arabian Sea, Open Ocean: MD 900963

At site MD 900963, TOC varies between 0.2 and 0.9 % during the last 330 kyr. Thus highest values are reached off Oman, and intermediate and lowest values are reached in the WAS and EAS, respectively. In the EAS, highest TOC (Figure 6) values are associated with glacial $\delta^{18}O$ maxima, and lower values are associated with interglacial minima every 20 to 25 kyr [*Rostek et al.,* 1994]. The TOC MAR (0.08 to 0.33 g/m^2 per year) follow the pattern of the TOC record, while the concentrations of C_{37} alkenones (243 to 6696 ng/g dry sediment) and C_{37} MAR (6 to 242 μg/m^2 per year) (Figure 6) also parallel these variations [*Rostek et al.,* 1994].

The results of the spectral analyses on TOC and TOC MAR (Figure 7) are in good accordance to GeoB 3005. Again, dominant variance is concentrated at the 23 kyr period [*Rostek et al.,* 1997] in both records, while TOC MAR, additionally, reveals a peak in the frequency band of eccentricity. Thus the 23 kyr periodicity is revealed in the WAS and EAS and at the continental margin off Oman, although with much lower importance at the coastal site.

5.4. Cross-Spectral Analysis

The results of the cross-spectral analyses (Figure 8) reveal differences in the frequency domain as well as in the phase relationship to boreal summer insolation for June 21 at 30°N

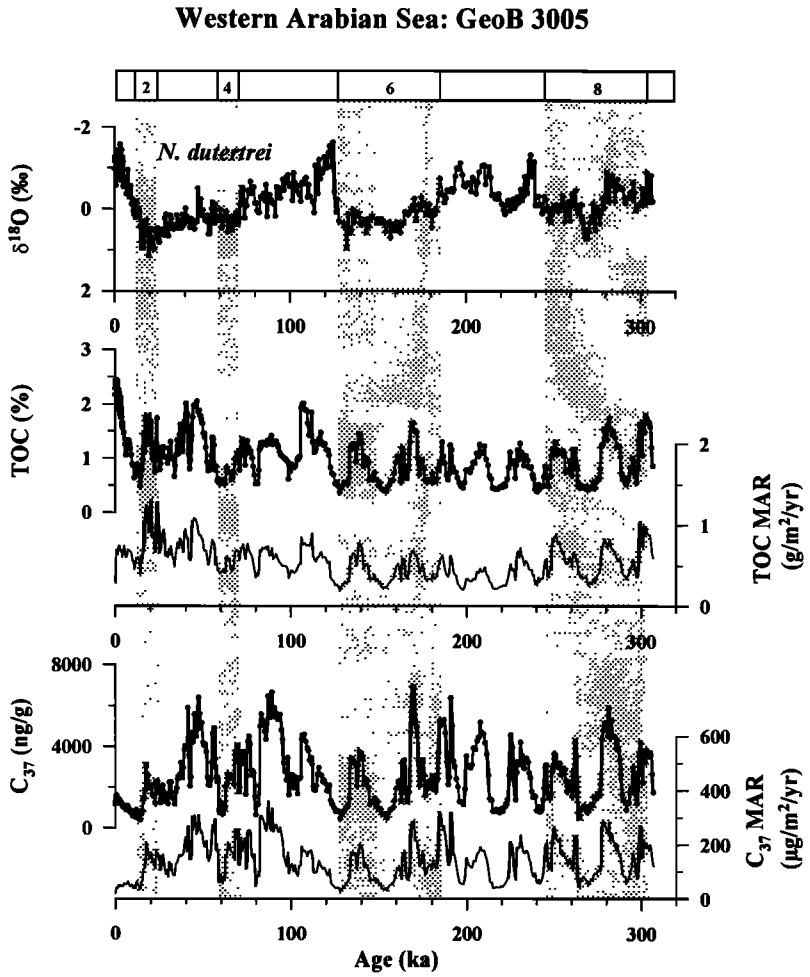

Figure 3. Time series of the $\delta^{18}O$ record of the planktonic foraminifera *Neogloboquadrina dutertrei*, total organic carbon (TOC) concentrations and mass accumulation rates (TOC MAR), and C_{37} alkenone concentrations (C_{37}) and mass accumulation rates (C_{37} MAR) for core GeoB 3005.

of all three cores in the WAS (GeoB 3005), at the continental slope off Oman (ODP Site 723), and in the EAS off the Maldives (MD 900963).

The 23 kyr cyclicity of GeoB 3005 (Figure 8a) is coherent (k = 0.9931) with boreal summer insolation but reveals a phase relationship of +11.3 kyr (+177°) (Table 2). This opposite phasing between summer insolation and TOC in GeoB 3005 is shown more illustratively in Figure 9.

ODP Site 723 (Figure 8b) exhibits strong variances in the low-frequency domain, which links TOC variations mainly to the glacial-interglacial cycles dominated by the 100 kyr period. However, a strong coherency (k = 0.9906) is still evident between boreal summer insolation and TOC time series within the precession band. The phase relationship of -11.4 kyr (-178°) is similar to that calculated for GeoB 3005 (Figure 9, Table 2).

The coherence between TOC of MD 900963 and boreal summer insolation (Figure 8c) is strong (k = 0.9609) in the precession band, but phase relationship reveals a 7.7 kyr (+120°) lead of TOC.

6. Discussion

With the availability of longer proxy records the precessional component of the Earth's parameters became evident in productivity changes all over the Arabian Sea, although with varying intensity [e.g., *Prell,* 1984; *Clemens and Prell,* 1990, 1991; *Shimmield et al.,* 1990; *Murray and Prell,* 1992; *Anderson and Prell,* 1993; *Emeis,* 1993; *Bassinot et al.,* 1994; *Rostek et al.,* 1997; *Altabet et al.,* 1995; *Reichart et al.,* 1998; *Schubert et al.,* 1998]. On the basis of biological, biogeochemical, and lithogenic evidence, *Clemens et al.* [1991] concluded that the response of the summer monsoon winds over the Arabian Sea to insolation changes is of more importance to the timing and wind strength than the glacial-interglacial climate variability. Additionally, *Sirocko et al.* [1993] discussed variations in the records of marine oxygen isotopes and carbonate and aeolian dust supply, which originated from Arabia and Mesopotamia by northwesterly winds, in relation with insolation changes in the WAS.

Recent studies suggest a coupling between increased biogenic as well as lithogenic particle fluxes, higher

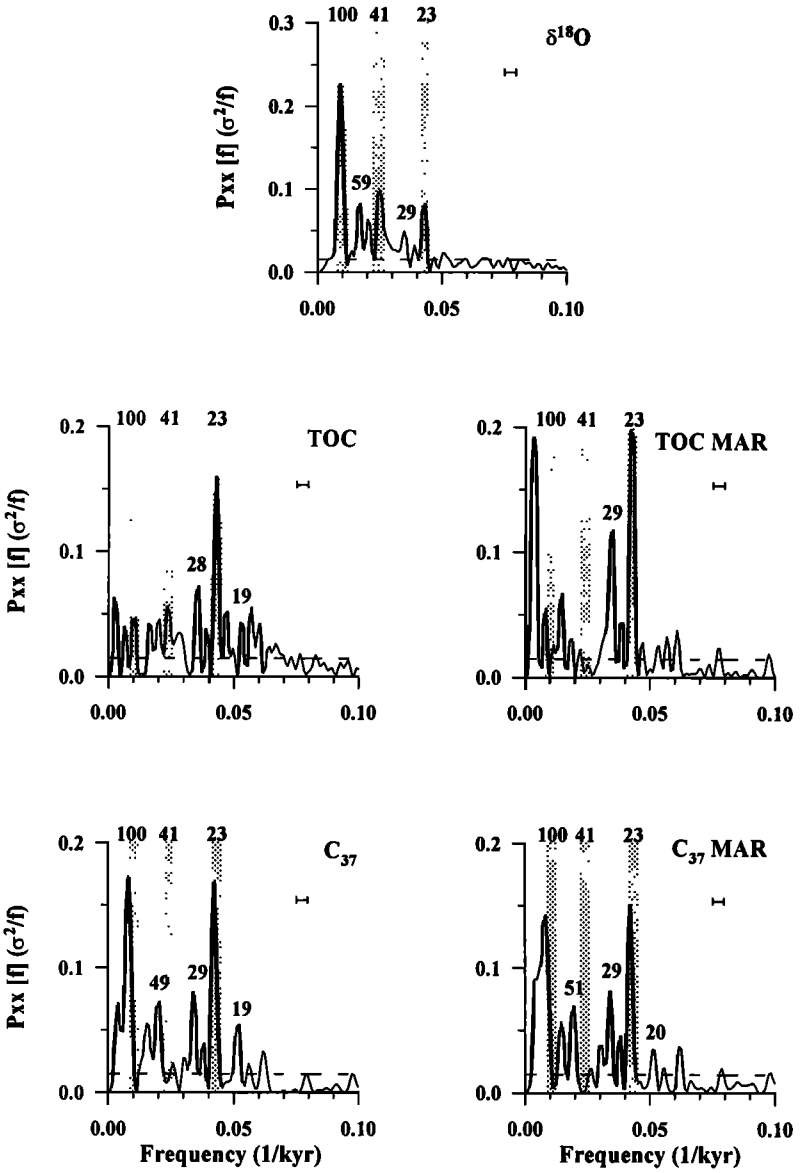

Figure 4. Results of harmonic analysis calculated on the $\delta^{18}O$, TOC, TOC MAR, C_{37} and C_{37} MAR records of GeoB 3005 using the software program SPECTRUM [*Schulz and Stattegger*, 1997]. A Fischer/Siegel test (dashed line) for compound periodicity was employed, and significant peaks outside the eccentricity (100), obliquity (41), and precession band (23) are labeled separately. Horizontal bar marks 6 dB bandwidth for each calculation.

SW monsoon wind speeds, and decreasing sea surface temperatures in the WAS and EAS [*Nair et al.*, 1989; *Ittekkot et al.*, 1992; *Haake et al.*, 1993]. Thus, if the SW monsoon wind strength responds directly to insolation changes, then biological, biogeochemical, and lithogenic proxies for paleoupwelling and wind intensity should be in phase with boreal summer insolation. However, numerous studies concerning the reconstruction of upwelling-related paleoproductivity in the Arabian Sea reveal a wide range of phase angles (-6.6 to +7.7 kyr) between the various proxies and boreal summer insolation [e.g., *Clemens and Prell*, 1990, 1991; *Shimmield et al.*, 1990; *Murray and Prell*, 1992; *Emeis*, 1993; *Altabet et al.*, 1995; *Beaufort et al.*, 1997; *Reichart et al.*, 1998]. This indicates that maxima in wind strength, paleoproductivity, and upwelling significantly deviate from maxima in boreal summer insolation at June 21. None of them even has a maximum within the half cycle of enhanced insolation. On the basis of their phase angles these proxies used to reconstruct monsoonal climate can be divided into three groups (Table 2, Figure 9) reflecting (1) summer monsoon wind strength and related upwelling intensity in the WAS (Group 1: -6.4 to -9.6 kyr), (2) paleoproductivity in the WAS (-10.9 to +9.6 kyr), and (3) paleoproductivity in the EAS (+8.3 to +6.4 kyr).

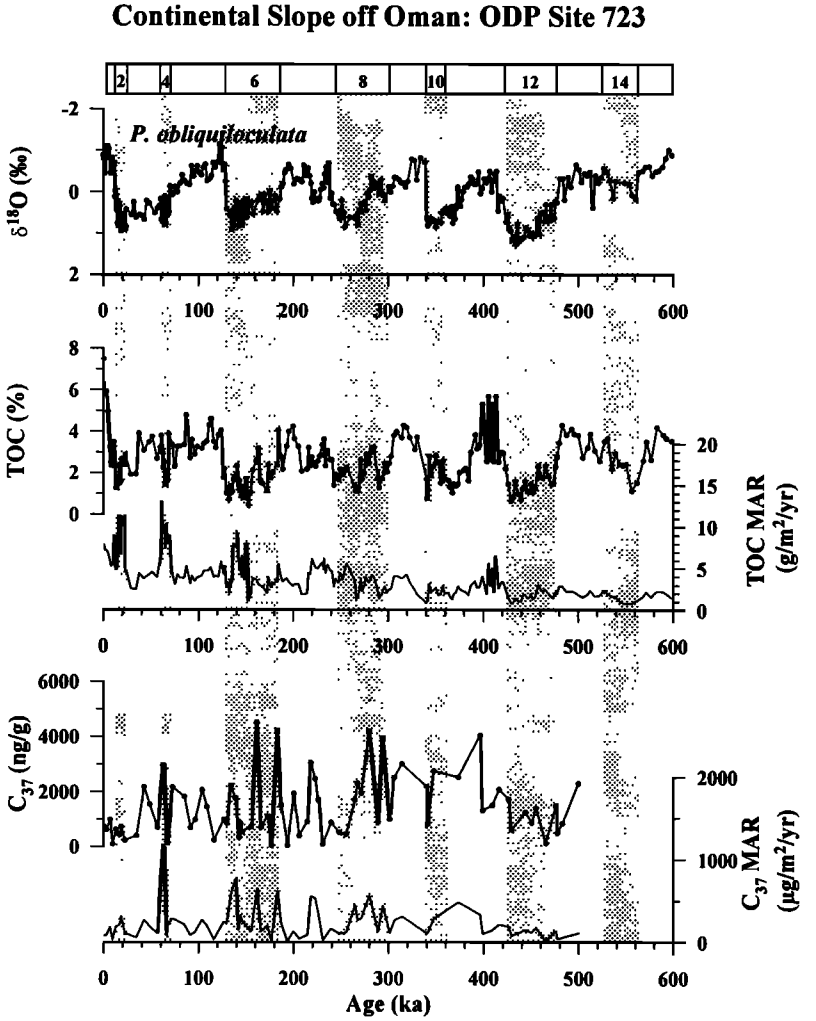

Figure 5. Time series of $\delta^{18}O$ of the planktonic foraminifera *Pulleniatina obliquiloculata*, TOC, TOC MAR, C_{37}, and C_{37} MAR for ODP Site 723 [*Nitsuma et al.*, 1991, *Emeis*, 1993, *Emeis et al.*, 1995]. Data was kindly provided by K.-C. Emeis

6.1. Group 1: SW Monsoon Wind Strength and Upwelling Intensity in the Western Arabian Sea (-6.4 to -9.6 kyr)

Clemens and Prell [1990] and *Clemens et al.* [1991] used marine and terrestrial proxies, giving independent information on marine biological processes and the timing of maxima in summer monsoon wind intensity. The marine proxies, consisting of the concentration of the planktonic foraminifera *Globigerina bulloides*, barium, and biogenic opal fluxes, reveal a strong coherency with boreal summer insolation but show phase lags of -8.7 (-121°), -6.6 (-104°), and -7.2 kyr (-113°), respectively, in the precession band. A grain size record was used as terrestrial indicator for the SW monsoon intensity, revealing a phase lag of -9.5 kyr (-148°) [*Clemens et al.*, 1991]. Together these proxies forming group 1 reveal a time lag of roughly 6 to 9 kyr, which was attributed to variations in the cross-equatorial transport of latent heat originating from the southern Indian Ocean and its release over the Asian Plateau, which according to the model of *Clemens et al.* [1991], determines the strength of the SW monsoon.

Altabet et al. [1995] used the sedimentary $^{15}N/^{14}N$ ratios to reconstruct denitrification intensity, the process by which nitrate is reduced to gaseous nitrogen species, an important limiting factor for marine productivity [*Altabet and Curry*, 1989]. In the precessional frequency band the $\delta^{15}N$ record from the Owen Ridge is coherent and nearly in phase with *G. bulloides* (percent) suggesting a strong link between denitrification and upwelling. Similar to the other records described above, $\delta^{15}N$ lags boreal summer insolation by 9 kyr (Table 2) [*Altabet et al.*, 1995] and thus belongs to group 1.

Reichart et al. [1998] applied an age model independent of the SPECMAP timescale, which reduced the phase lag between monsoon proxies and summer insolation by 2 kyr. In spite of this alternative chronology tuned to the $\delta^{18}O$ timescale of MD 84641 [*Lourens et al.*, 1996] from the Mediterranean a time lag between the productivity proxies *G. bulloides* (percent) and TOC with respect to early summer insolation of 6 to 7.5 kyr (Table 2) is still evident. This was attributed by the authors to a prolonged upwelling season caused by an increased insolation during August and September, suggesting that the length of the summer monsoon

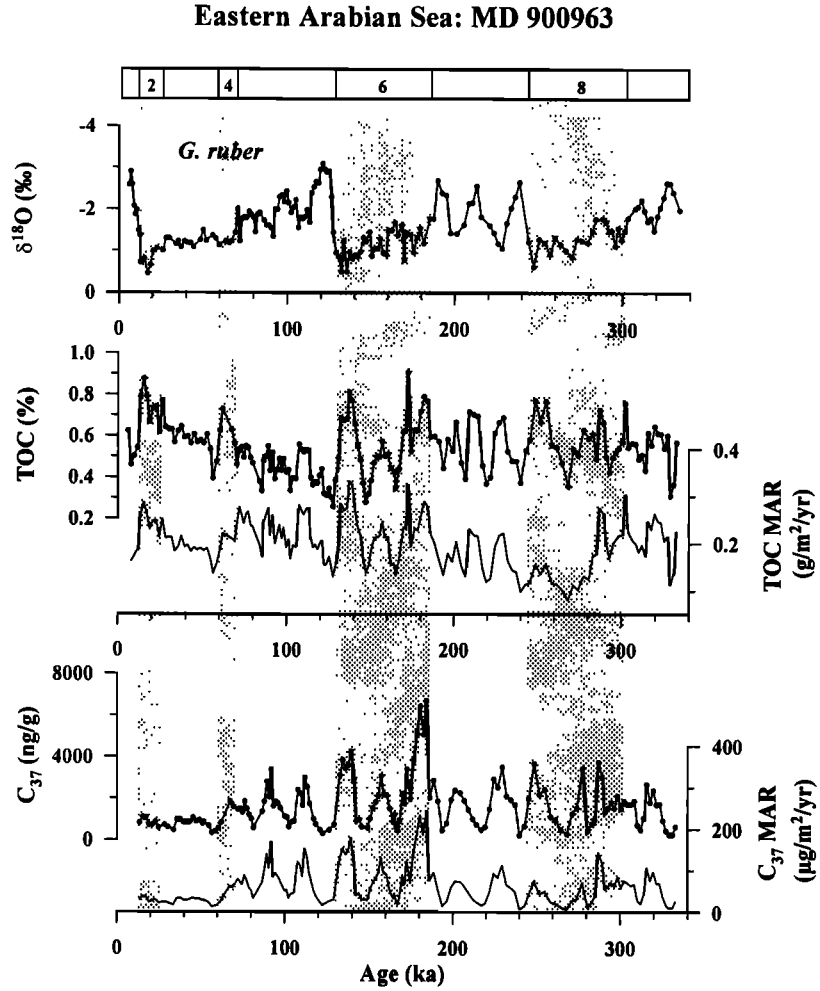

Figure 6. Time series of $\delta^{18}O$ of the planktonic foraminifera *Globigerinoides ruber*, TOC, TOC MAR, C_{37} and C_{37} MAR for MD 900963 [*Rostek et al.*, 1994, 1997].

is more important to annual fluxes of *G. bulloides* and TOC than the wind strength at the time of early summer insolation maximum.

6.2. Group 2: Paleoproductivity in the Western Arabian Sea (-10.9 to +9.6 kyr)

Group 2, consisting only of records of TOC and C_{37} alkenones, reveals opposite phasing between -10.9 and +9.6 kyr to boreal summer insolation maxima in the precessional frequency band (Table 2, Figure 9). *Murray and Prell* [1992] described similar opposite relationships of +10 kyr (~ +157°) (Table 2) between maxima of TOC, TOC MAR, and estimates of paleoproductivity, inferred from the sedimentary TOC content after *Müller and Suess* [1979], and maxima in Northern Hemisphere summer insolation. In their study the phase of TOC and productivity records lie directly between the phasing of indicators for summer monsoon strength at about -7.7 kyr (-120°) on average (group 1) and that of high sedimentation rates associated with lithogenic input at 5.8 kyr (+90°) in phase with maximum ice volume. From this they concluded that either the TOC signal reflects preservation changes due to enhanced sedimentation rates or the production of organic carbon is not directly linked to monsoonal upwelling.

Variations in TOC and the C_{37} alkenone concentrations may be attributed to changes in either productivity or preservation. Today, the Arabian Sea is characterized by a pronounced oxygen minimum zone (OMZ) between 150 and ~ 1500 m [*Wyrtki*, 1971], initiating a controversial discussion about its influence on proxies used to reconstruct paleoproductivity, especially sedimentary TOC. Higher sedimentary TOC contents may be the result of generally higher export production rates and a probably somewhat better preservation of organic matter settling through a stronger OMZ. *Paropkari et al.* [1992] compared the sedimentary TOC contents on the continental slopes of the Indian margin and the Arabian Peninsula. They inferred that bottom water anoxia plays an important role on the sedimentary TOC concentrations. In contrast, *Pedersen et al.* [1992] examined the 0 to 1 cm depth interval from 14 undisturbed box cores collected from the outer shelf-upper continental slope area off Oman from water depths < 1650 m.

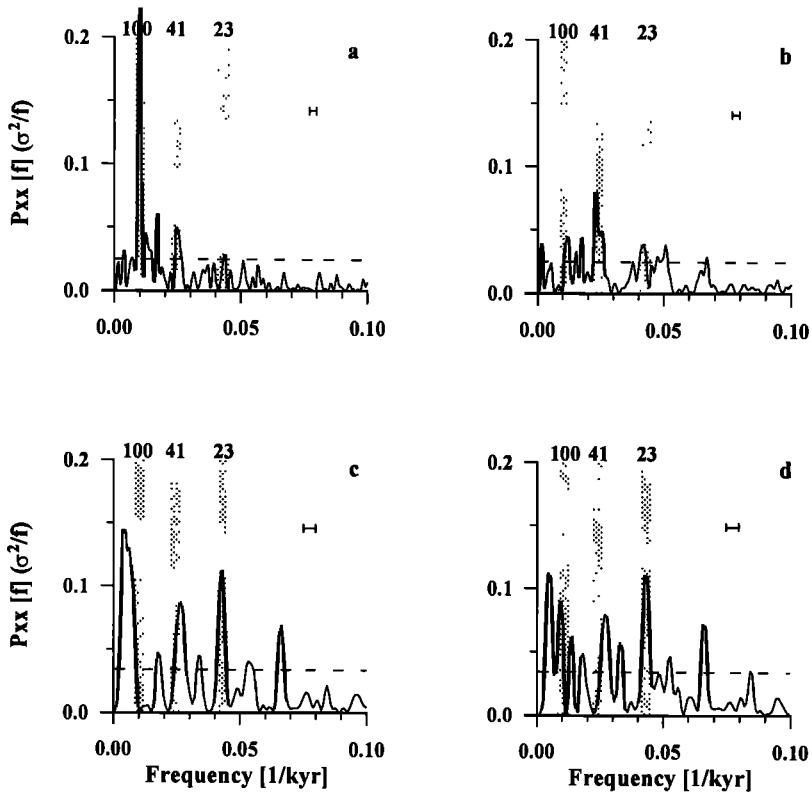

Figure 7. Results of harmonic analysis calculated on (a) TOC and (b) TOC MAR of ODP Site 723 [*Emeis*, 1993, *Emeis et al.*, 1995] and (c) TOC and (d) TOC MAR of core MD 900963 [*Rostek et al.*, 1994, 1997] using the software program SPECTRUM [*Schulz and Stattegger*, 1997]. A Fischer/Siegel test (dashed line) for compound periodicity was employed, and significant peaks outside the eccentricity (100), obliquity (41), and precession band (23) are labeled separately. Horizontal bar marks 6 dB bandwidth for each calculation.

Their findings suggested that there is little relationship between the bottom water oxygen concentration and the sedimentary content of marine organic matter on the Oman margin.

Reichart et al. [1998] compared TOC patterns in cores from different water depths in the northern Arabian Sea. They found that TOC fluctuations in cores from within and below the OMZ can be correlated one by one with each other, although TOC contents are lower in the deep water cores, and concluded that variations in TOC are not caused by fluctuations in the OMZ but are primarily controlled by changes in surface water productivity. Additionally, *Schubert et al.* [1998] examined several organic biomarker compounds, such as alkenones in relation with variations of TOC over the past 200 kyr. They confirmed the use of alkenones, TOC, and other organic biomarkers as qualitative indicators for paleoproductivity changes in Arabian Sea sediments.

While *Paropkari et al.* [1992] suggest that bottom water anoxia plays an important role on the sedimentary TOC concentrations, several other studies indicate that variable bottom water oxygen concentrations in the OMZ have only little or no effect on TOC variations in the Arabian Sea [e.g., *Pedersen et al.*, 1992; *Reichart et al.*, 1998; *Schubert et al.*, 1998]. *Rostek et al.* [1994, 1997] assumed that variations of organic matter are related to changes in marine productivity in the WAS and EAS. They used the distribution of the coccolithophorid species *F. profunda* as a proxy to estimate variations in surface productivity. High TOC contents and alkenone concentrations are accompanied by a low ratio of *F. profunda* to total coccoliths, indicating a shallow thermocline and enhanced surface water productivity. This is corroborated by transfer functions based on coccolithophorids [*Beaufort et al.*, 1997] and planktonic foraminifera [*Cayre et al.*, 1999] at site MD 900963. Additionally, different kinds of organic biomarker compounds [*Schulte et al.*, 1999] and redox-sensitive trace metals [*Pailler et al.*, 1998] revealed that the bottom waters remained oxygenated during the last 330 kyr at site MD 900963. Intense bioturbation throughout the whole core indicates oxygenated bottom water conditions at site GeoB 3005 [*Hemleben et al.*, 1996]. The good agreement between the TOC and TOC MAR, as well as between C_{37} and C_{37} MAR records in both GeoB 3005 and MD 900963 indicates that variations in these records reflect changes in surface water productivity rather than preservation changes due to varying sedimentation rates [*Müller and Suess*, 1979].

In contrast, dilution effects due to higher sedimentation rates of terrigenous lithogenic material and preservation as an additional controlling factor on TOC and C_{37} cannot be excluded at ODP Site 723. The higher TOC concentrations during interglacial times at ODP Site 723 are corroborated by a *G. bulloides* record [*Emeis et al.*, 1995] also indicating

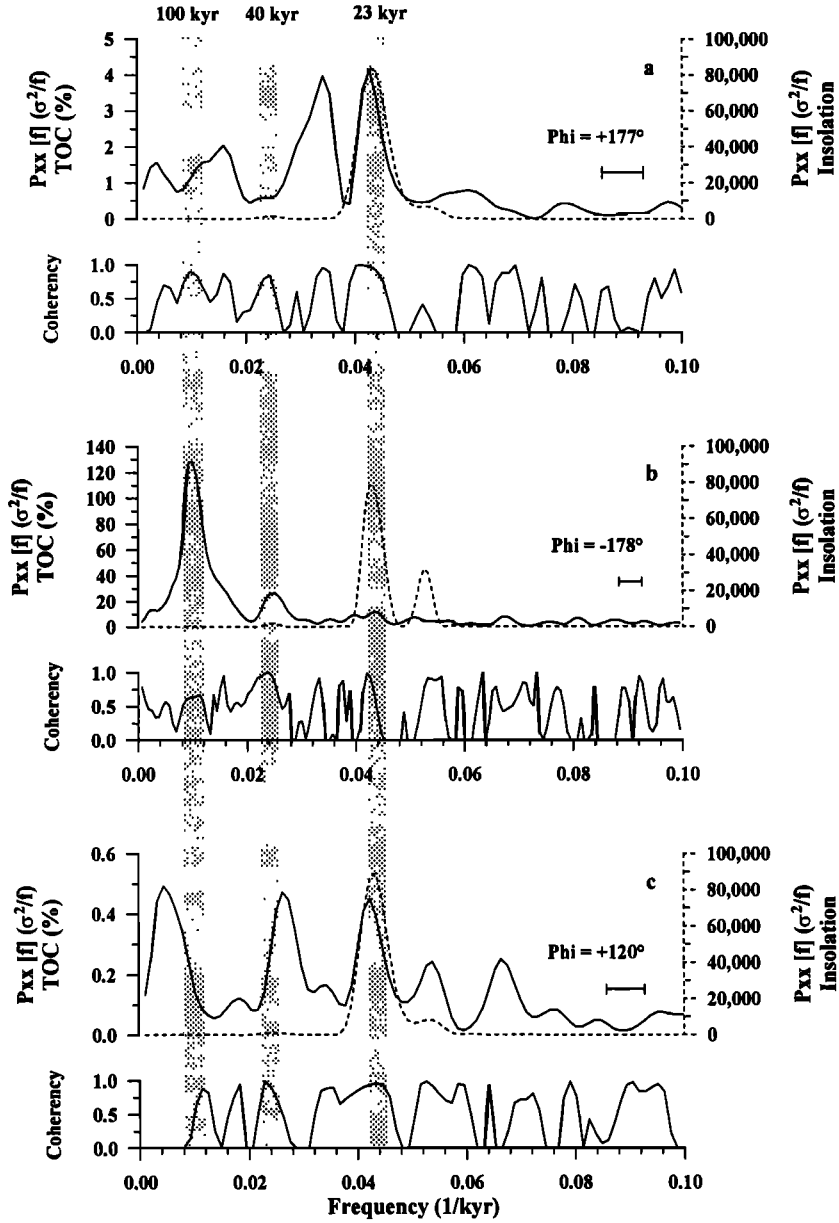

Figure 8. Results of the cross-spectral analyses between boreal summer insolation (June 21, 30°N) calculated after *Berger* [1978] using the AnalySeries software package [*Paillard et al.*, 1996] and TOC records of (a) GeoB 3005, (b) ODP Site 723 [*Emeis*, 1993; *Emeis et al.*, 1995], and (c) MD 900963 [*Rostek et al.*, 1994, 1997] applying the software program SPECTRUM [*Schulz and Stattegger*, 1997]. Horizontal bar marks 6 dB bandwidth for each calculation.

higher productivity levels during interglacial times. Thus *Emeis et al.* [1995] suggested TOC to be a more suitable indicator of productivity than accumulation rates at this site.

The results of the cross-spectral analyses of GeoB 3005 and ODP Site 723 described in this study (Table 2, Figure 9) are in good agreement with *Emeis* [1993] and *Murray and Prell* [1992], who calculated the paleoproductivity rates after *Sarnthein et al.* [1992] or *Müller and Suess* [1979] using TOC MAR at ODP Site 723 and RC27-61, respectively. These calculations revealed a phase relationship to boreal summer insolation of about +10.5 kyr (+165°) (Table 2). We therefore assume that variations of TOC in the precessional frequency domain in the WAS can be attributed to productivity rather than to preservation changes. To explain the opposite phasing, we propose that variations of paleoproductivity indicated by TOC, alkenones, and other organic biomarkers are not directly linked to maximum monsoonal upwelling intensity and wind strength in the WAS.

6.3. Group 3: Paleoproductivity in the Eastern Arabian Sea (+8.3 to +6.4 kyr)

Group 3 summarizes phase angles between +8.3 (+130°) and +6.4 kyr (+100°) (Figure 9) in phase with maximum precessional ice volume. The leading of productivity records of site MD 900963 of +7.7 kyr (+120°) on average (Table 2)

Table 2. Summary of Phase Angles Between Time Series of Different Cores and Precessional Insolation (June 21)

	Author (s)	Core	Time Series	Precession (June 21)	
				Phase, deg.	Lead/Lag, kyr
Group1	*Clemens et al.* [1991]	ODP Site 722	Opal MAR	-113 +/-21	7.2 +/-1.3
			Ba flux	- 04 +/-10	6.6 +/-0.6
		RC27-61	*G. bulloides* (%)	-121 +/-23	8.7 +/-1.3
			Lithogenic Grain Size	-148 +/-12	9.5 +/-0.6
Group1	*Altabet et al.* [1995]	RC27-61	d15N	-141 +/-20	9.0 +/-1.3
Group1	*Reichart et al.* [1998]	NIOP 464	*G. bulloides* (%)	-103 +/-31	6.6 +/-2.0
			TOC (%)	-116 +/-29	7.4 +/-1.9
Group 2	*Murray & Prell* [1992]	RC27-61	TOC (%)	+170 +/-25	10.9 +/-1.6
			TOC MAR	+155 +/-15	9.9 +/-1
			PP estimates [*Müller and Suess*, 1979]	+162 +/-28	10.4 +/-1.8
Group 2	*Emeis* [1993]	ODP Site 723	PP estimates [*Sarnthein et al.*, 1992]	+167 +/-27	10.7 +/-1.7
Group 2	this study	GeoB 3005	TOC (%)	+177 +/-4	11.3 +/-0.3
			TOC MAR	+173 +/-4	11.1 +/-0.3
			C_{37} (ng/g)	+172 +/-7	11 +/-0.4
			C_{37} MAR	+168 +/-6	10.7 +/-0.4
Group 2		ODP Site 723	TOC (%)	-178 +/-5	11.4 +/-0.3
			TOC MAR	+153 +/-6	9.8 +/-0.4
Group 3	*Beaufort et al.* [1997]	MD 900963	PP (*F. profunda*)	+118	7.5
Group 3	this study		TOC (%)	+120 +/-10	7.7 +/-0.6
			TOC MAR	+129 +/-8	8.2 +/-0.5
			C_{37} (ng/g)	+108 +/-2	6.9 +/-0.1
			C_{37} MAR	+110 +/-4	7 +/-0.3

Positive values indicate a lead with respect to insolation maximum, whereas negative values indicate a lag. A detailed description of the age models and cross-spectral analyses of MD 900963, NIOP 464, ODP Site 723, RC27-61, and ODP Site 722 are given by *Bassinot et al.* [1994] (age model) and *Beaufort et al.* [1997] (cross-spectral analysis), *Reichart et al.* [1998], *Emeis* [1993], and *Clemens and Prell* [1990] and [1991], respectively. The proxies were divided into three groups reflecting summer monsoon wind strength and related upwelling intensity in the western Arabian Sea (WAS) (-6.4 to -9.6 kyr) and paleoproductivity in the WAS (-10.9 to +9.6 kyr) and eastern Arabian Sea (+8.3 to +6.4 kyr).

is consistent with the previously published work of *Beaufort et al.* [1997]. They used the relative abundance of the coccolithophorid *F. profunda* as a marker for variations in primary productivity for the past 910 kyr at site MD 900963. *Beaufort et al.* [1997] suggested that productivity in the EAS is coherent and in phase with the early spring equatorial insolation and therefore is related to the wind intensity of the westerlies.

On the other hand, *Rostek et al.* [1994, 1997] inferred a link between precession-dominated paleoproductivity and deeper mixing due to stronger and predominating NE monsoons during glacial times in the EAS on the basis of higher TOC and C_{37} alkenone contents during glacial interstadials. Additionally, recent studies suggested that the NE monsoon winds are responsible for deepening of the mixed layer, thereby injecting nutrient-rich subsurface waters into the photic zone [*Rao et al.*, 1989]. According to *Emeis et al.* [1995], an expanded and thickened snow cover over the Tibetan Plateau may have at least prolonged the NE monsoon season. Consequently, in the EAS, paleoproductivity seems to be predominantly linked to variations in the NE monsoon winds, which are probably related to maximum precessional ice volume.

6.4. Implications for the Sedimentary TOC and C_{37} Alkenone Signal in the Arabian Sea

Although *Clemens et al.* [1991] attributed the 6 to 9 kyr time lag between proxies belonging to group 1 and boreal summer insolation to variations in the cross-equatorial transport of latent heat, the TOC and C_{37} signals from the WAS and EAS indicate that the SW monsoon and related upwelling intensity alone cannot account for the different

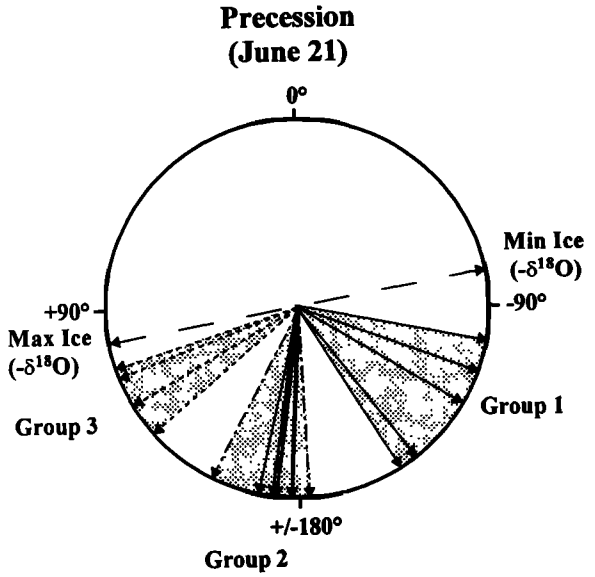

Figure 9. Precessional phase wheel summarizing proxies of group 1 (-6.4 to -9.6 kyr) used to reconstruct SW monsoon wind intensity and related upwelling in the WAS [*Clemens and Prell*, 1990; *Clemens et al.*, 1991; *Altabet et al.*, 1995] referenced to maximum insolation corresponding to June 21. Groups 2 (-10.9 to +9.6 kyr) and 3 (+8.3 to +6.4 kyr) indicate productivity proxies (TOC, TOC MAR, C_{37}, and C_{37} MAR) from cores GeoB 3005 (solid line) as well as from ODP Site 723 (long- and short-dashed line) and MD 900963 (dashed line) in the WAS and EAS, respectively, calculated in this study.

phasing of groups 1, 2, and 3. The explanations of group 1, cross-equatorial transport of latent heat [*Clemens et al.* 1991], and prolonged summer monsoon season [*Reichart et al.*, 1998] cannot be resolved here. The timing of groups 2 and 3 between maxima in the monsoon indices of group 1 and maximum ice cover leading insolation at June 21 by about +6.4 kyr (+100°) (Figure 9) implies a pronounced influence of the NE monsoon winds on TOC and C_{37} fluxes in the WAS and EAS. According to *Prell* [1984], a stronger snow cover over Asia delays the onset and shortens the summer monsoon season. Thus a prolonged NE monsoon due to minimum summer insolation and increased ice volume may have lead to a deepening of the mixed layer enhancing the primary productivity and particle fluxes in the WAS and EAS [*Nair et al.*, 1989; *Rao et al.*, 1989] rather than inducing stronger upwelling. A strengthening and prolongation of the NE monsoon season, increasing the vertical mixing during boreal winter at times opposite to maxima in precessional summer insolation, were previously proposed by *Van Campo et al.* [1982] and *Emeis et al.* [1995].

Additionally, recent studies of *Rixen et al.* [1996] suggest that during periods of strong SW monsoon winds, cold, nutrient-depleted, south equatorial water is transported to the north into the WAS, where these water masses reduce the amount of nutrients, thereby diminishing productivity related biogenic particle fluxes. Thus highest flux rates associated with upwelling occur during SW monsoons of minor to intermediate strength [*Rixen et al.*, 1996]. Consequently, variations in paleoproductivity in the WAS are probably linked to deeper mixing of surface waters through the action of stronger and prolonged NE monsoon winds [*Emeis et al.*, 1995] and to rather moderate SW monsoon intensity, as suggested by recent studies of *Rixen et al.* [1996]. In the EAS the TOC and alkenone maxima are in phase with maximum ice volume, indicating an additional influence of stronger and prolonged NE monsoon winds associated with cold climates, as proposed by *Rostek et al.* [1994, 1997].

7. Conclusions

Variations in the sedimentary content of TOC and C_{37} at sites GeoB 3005 and MD 900963 reveal a dominating 23 kyr cyclicity, indicating a precession-related insolation forcing on paleoproductivity in the WAS and EAS. It is worth noting that while in the EAS variance in the frequency domain of eccentricity is present in TOC MAR associated with interstadials in glacial $\delta^{18}O$ maxima [*Rostek et al.*, 1994, 1997], the record from the western regions is exclusively characterized by the precession component. In contrast, ODP Site 723 exhibits strong variance in the eccentricity band [*Emeis*, 1993], showing higher TOC values during interglacial periods at the continental slope off Oman [*Emeis et al.*, 1995]. Superimposed on these fluctuations in the low-frequency domain are variations in the precession band at ODP Site 723.

According to their phasing related to precessional variations in boreal summer insolation, referenced to June 21, monsoonal indices as well as paleoproductivity proxies can be divided into three groups reflecting summer monsoon wind strength and related upwelling intensity in the WAS (group 1: -6.4 to -9.6 kyr) and paleoproductivity in the WAS (group 2: -10.9 to +9.6 kyr), and EAS (group 3: +8.3 to +6.4 kyr). Cross-spectral analyses reveal a coherent but opposite phase relationship of TOC records of GeoB 3005 and ODP Site 723 with respect to Northern Hemisphere summer insolation. These productivity-related proxy records lie directly between the indicators for SW monsoon wind strength and related upwelling intensity as described by *Clemens et al.* [1991] belonging to group 1, and maximum ice volume, which probably prolongs and strengthens the NE monsoon winds. TOC of MD 900963 leads summer insolation by +7.7 kyr (group 3) thus is very close to maximum ice volume in the precession band.

We interpret the maxima in TOC and C_{37} alkenone variations to be a combined signal of moderate SW monsoon wind strength, as suggested by *Rixen et al.* [1996], and additionally strengthened and prolonged NE monsoon winds enhancing primary productivity due to deeper mixing in the WAS, while paleoproductivity seemed to predominantly correspond to the NE monsoon winds in the EAS.

Acknowledgments. We thank Hella Buschhoff, Dietmar Grotheer, and Ralph Kreutz for technical assistance in the home laboratory; the officers, crew, and scientists aboard *R/V Meteor* for their help with coring and sampling operations; the Ocean Drilling Program (ODP) and Kai-Christian Emeis for providing data from ODP Site 723. This research was funded by the Deutsche Forschungsgemeinschaft and the Bundesminister für Bildung und Forschung (BMBF), Bonn. Paleoclimate work at CEREGE is supported by CNRS (PNEDC), the European Community (projects ENV4-CT97-0564, FMRX-CT96-0046, and ENV4-CT97-0659), and the IFCPAR (project 1809-1). Previous versions of this manuscript greatly benefited from reviews by M. Delaney, G.J. Reichart, and an anonymous reviewer. The data of GeoB 3005 presented in this paper will be archived in the Pangaea database (www.pangaea.de/Projects/SFB261/DBudziak_et_al_2000/).

References

Altabet, M. A., and W. B. Curry, Testing models of past ocean chemistry using foraminifera $^{15}N/^{14}N$, *Global Biogeochem. Cycles, 3,* 107-119, 1989.

Altabet, M. A., R. Francois, D. W. Murray, and W. L. Prell, Climate-related variations in denitrification in the Arabian Sea from sediment $^{15}N/^{14}N$ ratios, *Nature, 373,* 506-509, 1995.

Anderson, D. M., and W. L. Prell, A 300 kyr record of upwelling off Oman during the late Quaternary: Evidence of the Asian southwest monsoon, *Paleoceanography, 8,* 193-208, 1993.

Bassinot, F. C., L. Beaufort, E. Vincent, L. D. Labeyrie, F. Rostek, P. J. Müller, X. Quidelleur, and Y. Lancelot, Coarse fraction fluctuations in pelagic carbonate sediments from the tropical Indian Ocean: A 1500-kyr record of carbonate dissolution, *Paleoceanography, 9,* 579-600, 1994.

Beaufort, L., Y. Lancelot, P. Camberlain, O. Cayre, E. Vincent, F. Bassinot, and L. Labeyrie, Insolation changes as a major control of equatorial Indian Ocean primary productivity, *Science, 278,* 1451-1454, 1997.

Berger, A. L., Long-term variations of daily insolation and Quaternary climatic change. *J. Atmos. Sci., 35,* 2362-2367, 1978.

Brock, J. C., and C. R. McClain, Interannual variability in phytoplankton blooms observed in the northwestern Arabian Sea during the Southwest Monsoon, *J. Geophys. Res., 97,* 733-750, 1992.

Cadet, D., Meteorology of the Indian summer monsoon, *Nature, 279,* 761-767, 1979.

Cayre, O., L. Beaufort, and E. Vincent, Paleoproductivity in the equatorial Indian Ocean for the last 260,000 yr: A transfer function based on planktonic foraminifera, *Quat. Sci Rev., 18,* 839-857, 1999.

Clemens, S. T., and W. L. Prell, Late Pleistocene variability of Arabian Sea summer monsoon winds and continental aridity: Eolian records from the lithogenic component of deep-sea sediments, *Paleoceanography, 5,* 109-145, 1990.

Clemens, S. C., and W. L. Prell, One million year record of summer monsoon winds and continental aridity from the Owen Ridge (Site 722), northwest Arabian Sea, *Proc. Ocean Drill Program, Sci. Results, 117,* 365-388, 1991.

Clemens, S., W. Prell, D. Murray, G. Shimmield, and G Weedon, Forcing mechanisms of the Indian Ocean monsoon, *Nature, 353,* 720-725, 1991

DeMenocal, P. B., and D. Rind, Sensitivity of Asian and African climate to variations in seasonal insolation, glacial ice cover, sea surface temperature, and Asian orography, *J. Geophys. Res., 98,* 7265-7287, 1993.

Emeis, K.-C., Geochemische Auftriebsindikatoren in Sedimenten des Nordwestlichen Arabischen Meeres. Habilarbeit, Christian-Albrechts-Universität, Kiel, Germany, 1993.

Emeis, K.-C., D. M. Anderson, H. Doose, D. Kroon, and D. Schulz-Bull, Sea-surface temperatures and the history of monsoon upwelling in the northwestern Arabian Sea during the last 500,000 years, *Quat. Res.,N.Y., 43,* 355-361, 1995.

Findlater, J., A major low level air current near the Indian Ocean during the northern summer, *Q. J. R Meteorol. Soc., 95,* 362-380, 1969.

Haake, B., V. Ittekkot, T. Rixen, V. Ramaswamy, R. R. Nair, and W. B. Curry, Seasonality and interannual variability of particle fluxes to the deep Arabian Sea, *Deep Sea Res., Part I, 40,* 1323-1344, 1993.

Hansell, D. A., and E. T. Peltzer, Spatial and temporal variations of total organic carbon in the Arabian Sea, *Deep Sea Res. Part II, 45,* 2171-2193, 1998.

Hastenrath, S., and P. J. Lamb, *Climatic Atlas of the Indian Ocean,* Univ. of Wisc. Press, Madison, 1979.

Hemleben, C., W. Roether, and P. Stoffers, *Östliches Mittelmeer, Rotes Meer, Arabisches Meer, Cruise No. 31, 30 December 1994 - 22 March 1995, METEOR-Berichte* 96-4, 282 pp., Universität Hamburg, Hamburg, Germany, 1996.

Imbrie, J., J. D. Hays, D. G. Martinson, A. McIntyre, A. C. Mix, J. J. Morley, N. G. Pisias, W. L. Prell, and N. J. Shackleton, The orbital theory of Pleistocene climate: Support from a revised chronology of the marine $\delta^{18}O$ record, in *Milankovitch and Climate, NATO ASI Ser., Ser. C,* vol. 126, part 1, edited by A. L. Berger, pp. 269-305, D. Reidel, Norwell, Mass., 1984.

Imbrie, J., A. McIntyre, and A. C. Mix, Oceanic response to orbital forcing in the Late Quaternary: Observational and experimental strategies, in *Climate and Geosciences,* edited by A. L. Berger et al., pp. 121-164, Kluwer Acad., Norwell, Mass., 1989.

Ittekkot, V., B. Haake, M. Bartsch, R. R. Nair, and V. Ramaswamy, Organic carbon removal in the sea: The continental connection, in *Upwelling System: Evolution Since the Early Miocene,* edited by C. P. Summerhayes et al., *Geol. Soc. Spec. Pub.*, 64, 167-176, 1992.

Jenkins, G. M., and D. G. Watts, *Spectral Analysis and Its Application,* Holden-Day, San Francisco, Ca., 1968.

Lourens, L. J., A. Antonarakou, F. J. Hilgen, A. A. M. Van Hoof, C. Vergnaud-Grazzini, and W. J. Zachariasse, Evaluation of the Plio-Pleistocene astronomical timescale, *Paleoceanography, 11,* 391-413, 1996.

Luther, M. E., J. J. O'Brien, and W. L. Prell, Variability in upwelling fields in the northwestern Indian Ocean, 1, Model experiments for the past 18,000 years, *Paleoceanography, 5,* 433-445, 1990.

Müller, P. J., and E. Suess, Productivity, sedimentation rate, and sedimentary organic matter in the oceans, I, Organic carbon preservation, *Deep Sea Res., Part A 26,* 1347-1362, 1979.

Müller, P. J., R. Schneider, and G. Ruhland, Late Quaternary PCO_2 variations in the Angola Current: Evidence from organic $\delta^{13}C$ and alkenone temperatures, in *Carbon Cycling in the Glacial Ocean: Constrains on the Ocean's Role in Global Change,* edited by R. Zahn et al., *NATO ASI Ser., Ser. I, 17,* 343-366, 1994.

Murray, D. W., and W. L. Prell, Late Pliocene and Pleistocene climatic oscillations and monsoon upwelling recorded in sediments from the Owen Ridge, northwestern Arabian Sea, in *Upwelling Systems. Evolution Since the Early Miocene,* edited by C. P. Summerhayes et al., *Geol. Soc. Publ., 64,* 301-321, 1992.

Naidu, P. D., and B. A. Malmgren, A high-resolution record of late Quaternary upwelling along the Oman Margin, Arabian Sea based on planktonic foraminifera, *Paleoceanography, 11,* 129-140, 1996.

Nair, R. R., V. Ittekkot, S. J. Manganini, V. Ramaswamy, B. Haake, E. T. Degens, B. N. Desai, and S. Honjo, Increased particle flux to the deep ocean related to monsoons, *Nature, 338,* 749-751, 1989.

Niitsuma, N., T. Oba, and M. Okada, Oxygen and carbon isotope stratigraphy at Site 723, Oman Margin, *Proc. Ocean Drill. Program, Sci. Results, 117,* 321-341, 1991.

Paillard, D., L. Labeyrie, and P. Yiou, Macintosh program performs time series analysis, *Eos Trans. AGU, 77* (39), 379, 1996.

Pailler, D., F. Rostek, E. Bard, A. van Geen, R. Mortlock, and Y. Zheng, Precession control on sedimentary burial of organic matter and redox sensitive metals in the tropical Indian Ocean, *Mineral. Mag., 62A,* 1122-1123, 1998.

Paropkari, A. L., C. Prakash Babu, and A. Mascarenhas, A critical evaluation of depositional parameters controlling the variability of organic carbon in Arabian Sea sediments, *Mar. Geol., 107,* 213-226, 1992.

Pedersen, T. F., G. B. Shimmield, and N. B. Price, Lack of enhanced preservation of organic matter in sediments under the oxygen minimum on the Oman Margin, *Geochim. Cosmochim. Acta, 56,* 545-551,1992.

Prell, W. L., Monsoonal climate of the Arabian Sea during the late Quaternary: A response to changing solar radiation, in *Milankovitch and Climate, NATO ASI Ser., Ser. C,* vol. 126, part 1, edited by A. L. Berger et al., pp. 349-366, D. Reidel, Norwell, Mass., 1984.

Prell, W. L., and J. E. Kutzbach, Monsoon variability over the past 150,000 years, *J. Geophys. Res., 92,* 8411-8425, 1987.

Prell, W. L., and J. E. Kutzbach, Sensitivity of the Indian monsoon to forcing parameters and implications for its evolution, *Nature, 360,* 647-652, 1992.

Rao, R. R., R. L. Molinari, and J. F. Festa, Evolution of the climatological near-surface thermal structure of the tropical Indian Ocean, 1, Description of mean monthly layer depth, and sea surface temperature, surface current, and surface meteorological fields, *J. Geophys. Res , 94,* 10,801-10,815, 1989.

Reichart, G. J., L. J. Lourens, and W. J. Zachariasse, Temporal variability in the northern Arabian Sea oxygen minimum zone (OMZ) during the last 225,000 years, *Paleoceanography, 13,* 607-621, 1998.

Rixen, T., B. Haake, and V. Ittekkot, Coupling between SW monsoon-related surface and deep ocean processes as discerned from continuous particle flux measurements and correlated satellite data, *J. Geophys. Res., 101,* 28,569-28,582, 1996.

Rostek, F., G. Ruhland, F. C. Bassinot, L. Beaufort, P. J. Müller, and E. Bard, Fluctuations of the Indian monsoon regime during the last 170,000 years: Evidence from sea surface temperature, salinity and organic carbon records, in *Global Change and Precipitation,* edited by M. Debois and F. Desalmand, *NATO ASI Ser., Ser. I, 26,* 27-51, 1994.

Rostek, F., E. Bard, L. Beaufort, C. Sonzogni, and G. Ganssen, Sea surface temperature and productivity records for the past 240 kyr in the Arabian Sea, *Deep Sea Res. Part II, 44,* 1461-1480, 1997.

Sarnthein, M., U. Pflaumann, R. Ross, R. Tiedemann, and K. Winn, Transfer functions to reconstruct ocean palaeoproductivity: A comparison, in *Upwelling Systems. Evolution Since the Early Miocene,* edited by C. S. Summerhayes et al., *Geol. Soc. Spec. Publ., 64,* 411-427, 1992.

Schubert, C. J., J. Villanueva, S. E. Calvert, G. L. Cowie, U. von Rad, H. Schulz, U. Berner, and H. Erlenkeuser, Stable phytoplankton community structure in the Arabian Sea over the past 200,000 years, *Nature, 394,* 563-566, 1998.

Schulte, S., F. Rostek, E. Bard, J. Rullkötter, and O. Marchal, Variations of oxygen-minimum and primary productivity recorded in

sediments of the Arabian Sea, *Earth Planet. Sci. Lett., 173*, 205-221, 1999.

Schulz, M., and K. Stattegger, Spectrum: spectral analysis of unevenly spaced paleoclimatic time series, *Comput. & Geosci., 23*, 929-945, 1997.

Shimmield, G. B., S. R. Mowbray, and G. P. Weedon, A 350 ka history of the Indian Southwest Monsoon: Evidence from deep-sea cores, northwest Arabian Sea, *Trans. Roy. Soc. Edingburgh Earth Sci., 81*, 289-299, 1990.

Sirocko, F., M. Sarnthein, H. Erlenkeuser, H. Lange, M. Arnold, and J.-C. Duplessy, Century-scale events in monsoonal climate over the past 24,000 years, *Nature, 364*, 322-324, 1993.

Sonzogni, C., E. Bard, F. Rostek, R. Lafont, A. Rosell-Melé, and G. Eglinton, Core-top calibration of the alkenone index vs sea surface temperature in the Indian ocean, *Deep Sea Res., Part II, 44*, 1445-1460, 1997.

Swallow, J. C., Some aspects of the physical oceanography of the Indian Ocean, *Deep Sea Res., 31*, 639-650, 1984.

Van Campo, E., J.-C. Duplessy, and M. Rossignol-Strick, Climatic conditions deduced from a 150-kyr oxygen isotope-pollen record from the Arabian Sea, *Nature, 296*, 56-59, 1982.

Verardo, D. J., P. N. Froelich, and A. McIntyre, Determination of organic carbon and nitrogen in marine sediments using the Carlo Erba NA-1500 Analyzer, *Deep Sea Res., 37*, 157-165, 1990.

Volkman, J. K., S. M. Barrett, S. I. Blackburn, and E. L. Sikes, Alkenones in Gephyrocapsa oceanica: Implications for studies of paleoclimate, *Geochim. Cosmochim Acta, 59*, 513-520, 1995

Webster, P. J., The elementary monsoon, in *Monsoons*, edited by J. S. Fein and P. L. Stephens, pp. 3-32, John Wiley, New York, 1987.

Wyrtki, K., *Oceanographic Atlas of the International Indian Ocean Expedition*, 531 pp., U.S. Govt. Print. Off., Washington D.C., 531 pp, 1971.

Wyrtki, K., Physical oceanography of the Indian Ocean, in *The Biology of the Indian Ocean* edited by B. Zeitschel and S. A. Gerlach, pp. 18-36, Springer-Verlag, New York, 1973.

E. Bard and F. Rostek, CEREGE, Université d'Aix-Marseille III et CNRS-UMR 6635, Europôle de l'Arbois, BP80, 13545, Aix-en-Provence, Cedex 4, France.

D. Budziak, P. J. Müller, R. R. Schneider, and G. Wefer, Fachbereich Geowissenschaften, Universität Bremen, Postfach 330 440, 28334 Bremen, Germany. (budziak@uni-bremen.de; pmueller@uni-bremen.de; rschneid@uni-bremen.de; gwefer@uni-bremen.de)

(Received July 30, 1999;
revised December 29, 1999;
accepted January 5, 2000.)